Solutions of Nonlinear Free Surface-Body Interaction with A Harmonic Polynomial Cell Method

Yan-Lin Shao* and Odd M. Faltinsen
Centre for Ships and Offshore Structures & Department of Marine Technology, NTNU,
NO-7491, Norway
shao.yanlin@ntnu.no and odd.faltinsen@ntnu.no (*Presenting author)

The applications of Computational Fluid Dynamic (CFD) based on Navier-Stokes equations in ship and offshore hydrodynamics are still limited due to the heavy computational time. Potential-flow models are much faster compared with typical CFD solvers. It appears natural to apply the CFD in the region where the non-potential-flow effects matter (e.g. viscous flow separation and local wave breaking), and to solve Laplace equations elsewhere (See for instance Colicchio et al. [1] and Kristiansen & Faltinsen [2]). Many free-surface problems involving large volume structures are dominated by potential flow effects in the whole water domain. The objective of this study is to find an efficient numerical method to solve the fully-nonlinear potential-flow problems with the presence of free surface and a body. The problems considered in this abstract are in 2D. However, the experiences should also be useful guidance in 3D studies.

It is a strong tradition in marine hydrodynamics for solving the Laplace equation by Boundary Element Method (BEM) instead of field solvers, e.g. Finite Element Method (FEM), Finite Difference Method (FDM) and Finite Volume Method (FVM). An argument has been that a BEM solver based on simple fundamental solution to Laplace equation only needs to distribute singularities with unknown strength on the boundaries of the computational domain. Wu & Eatock Taylor [3] were perhaps the first in our field to give credit to the FEM-based field solver. Their comparison between FEM and BEM for a fully-nonlinear wave making problem suggests that FEM is more efficient than BEM in terms of both CPU time and computer memory. The memory required by a conventional BEM is O(N^2). Here N is the number of unknowns on the boundaries of the computational domain. A direct method such as the Gaussian elimination or LU-factorization takes O(N^3) operations in order to solve the resulting matrix equation. Typical iterative solvers, e.g. the Gauss-Seidel method and the Krylov subspace Generalized Minimal Residual (GMRES), would yield O(N^2) operation counts and consequently O(N^2) CPU time. Therefore, both CPU time and required memory for conventional BEM increase dramatically with increasing number of unknowns, which was considered as the bottleneck of the BEMs. Recent developments in BEM showed that the bottleneck of the BEMs no longer exist if the accelerated matrix-free methods, e.g. the pre-corrected Fast Fourier Transform method (*p*FFT) and the fast multipole method (FMM), are combined with the BEM solvers. Asymptotically, the *p*FFT method needs O(*NlogN*) memory and O(*NlogN*) CPU time, and the FMM needs O(*NlogN*) memory and O(*N*) CPU time. According to the authors' knowledge in the field of marine hydrodynamic, no direct comparative study has been made between the field solvers and the accelerated BEM solvers.

In the first part of the abstract, we study a mixed Dirichlet-Neumann Boundary Value Problem (BVP) in a 2D rectangular box by five different methods, two of which are BEM-based and the other three are categorized as field solvers. The size of the rectangular box is chosen as the same as studied by Wu & Eatock Taylor [3] in their wave making problem. The box length L is 40 times the box height h. See the definition in Fig.1. The Dirichlet boundary condition on the top surface and the Neumann boundary condition on the rest of the surfaces are given by the velocity potential function

$$\phi = \cosh\left[k(y+h)\right]\sin\left(kx\right). \qquad (1)$$

Here k is the wave number. h is the depth of the tank. x and y are the horizontal and vertical coordinates. The origin of the coordinate is located at the mid-point of the top surface with positive y-axis pointing upwards. The considered methods are a conventional constant BEM, a FMM accelerated constant BEM (FMM-BEM), a FVM and our two newly developed field solver based on Lagrangian Polynomial Cells (LPC) and Harmonic Polynomial Cells (HPC), respectively. The constant BEM code and FMM accelerated constant BEM code are based on open source codes with their basis explained in Liu & Nishimura [4]. The cell-centered control volumes are used to discrete the fluid domain in the FVM method adopted in this study. Some key features of the present FVM are summarized as follows: The integrations on the faces of the control volumes are approximated by midpoint rule; A linear reconstruction technique following [5] is applied for the approximation of the velocities and the velocity potential at the midpoint of the faces; The velocity at the center of the control volume is calculated by Gauss divergence theorem. The present FVM is second-order accurate with a uniform grid resolution.

Lagrangian Polynomial Cell (LPC) method: The idea of the present Lagrangian Polynomial Cell (LPC) method follow from the Lagrangian elements used in FEM (see e.g. Chung [6]). The desired interpolation functions of Lagrangian elements are constructed simply by a tensor product of the one-dimensional counterpart of x and y directions, respectively. We define a cell that contains 9 nodes, as shown in Fig.2. Node *1-8* are on the boundaries of the cell while node 9 is in the cell. We assume the distribution of the velocity potential can be approximated by polynomials. For simplicity and without loss of generality, we assume the origin of the coordinate system has the same location as point *9* of the cell. The velocity potential within the cell is approximated as

$$\phi(x,y) = a_1 + a_2 x + a_3 y + a_4 xy + a_5 x^2 + a_6 y^2 + a_7 xy^2 + a_8 x^2 y + a_9 x^2 y^2 \quad (2)$$

Plugging $\phi = \phi_j$, $x = x_j$ and $y = y_j$ (j=1,...,9) into the above equation, one obtains the unknown coefficients a_j (j=1,...,9) as the linear combinations of ϕ_j (j=1,...,9). For the nodes in fluid but not on boundaries, the Laplace equation is enforced by analytically taking $\left(\partial^2/\partial x^2 + \partial^2/\partial y^2\right)$ on both sides of Eq.(2). The Dirichlet and Neumann boundary conditions are satisfied in similar way with the assistance of Eq.(2). The considered LPC method has second-order accuracy.

Harmonic Polynomial Cell (HPC) method: The Harmonic Polynomial Cell method uses the harmonic polynomials as the basis of the interpolation functions. The harmonic polynomials satisfy Laplace equation. They are in two dimensions given by the real and imaginary parts of $(x+iy)^n$, where n is an integer. Therefore, we assume the following interpolation function

$$\phi(x,y) = b_1 + b_2 x + b_3 y + b_4\left(x^2 - y^2\right) + b_5 xy + b_6\left(x^3 - 3xy^2\right) + b_7\left(3x^2 y - y^3\right) + b_8\left(x^4 - 6x^2 y^2 + y^4\right) \quad (3)$$

Plugging $\phi = \phi_j$, $x = x_j$ and $y = y_j$ (j=1,...,8) into Eq.(3), the unknown coefficients b_j (j=1,...,8) can be found as the linear combinations of ϕ_j (j=1,...,8). This is equivalent to consider a sub Dirichlet boundary-value problem in the cell with Laplace equation as the governing equation. The boundary conditions are given on a set of discrete nodes on the boundaries , i.e. the edges of the cells. That is the reason we do not use information on points in the cell, e.g. point 9, to construct the interpolation functions. The solution at point 9 is equal to the interpolated value by Eq.(3), i.e. $\phi(x = x_9, x = y_9) = \phi_9$. The information on point 9 is used by the neighbor cells as illustrated by an example in Fig.2, where point 9 is on the boundary of the neighbor cell centered at point 5. The local indices of the points of the neighbor cell are marked with prime in Fig.2. This technique then provide continuity of the flow. The Dirichlet and Neumann boundary conditions are enforced by using Eq.(3) and its normal derivative on the boundary nodes, respectively. Note that Eq.(3) contains all the 3rd order harmonic polynomials and one 4th order polynomial term. Another 4th order harmonic polynomial term $\left(x^3 y - xy^3\right)$ was not included. It is beneficial to have higher-order terms in order to reduce the wave dispersion errors in the time-domain analysis.

The boundary elements used in the BEM and FMM-BEM analysis are uniformly distributed on both horizontal and vertical surfaces. Ny constant elements are distributed on each of the vertical boundary and $Nx = 40Ny$ elements on each horizontal boundary. Correspondingly, $(Nx \cdot Ny)$ square meshes are used in the field solvers, i.e. FVM, LPC method and HPC method. Hence the mesh size in x-direction Δx and that in y-direction Δy are $\Delta x = \Delta y = L/Nx = h/Ny$. All the methods in the comparison use the iterative GMRES solver. The residual error to stop the iterations is set to 0.5E-8 in GMRES. Proper preconditioners are used in order to achieve fast convergence. Fig.3 shows the CPU time for the five different solvers. The results are plotted against number of unknowns corresponding to constant BEM and FMM-BEM. It clear that the conventional BEM takes more CPU time than the FMM-BEM and all the three field solvers. This is in agreement with Wu & Eatock Taylor [3] who compared FEM and conventional BEM. We also noted that FMM-BEM performs best in terms of CPU time with the mesh resolution.

The accuracy of the methods are depicted in Fig.4 and Fig.5 by comparing the L_2 errors, which are defined as

$$e_{L2} = \sqrt{\sum_{i=1}^{N}\left(f_i^{num} - f_i^{an}\right)^2 \Big/ \sum_{i=1}^{N}\left(f_i^{an}\right)^2}\,. \quad (4)$$

Here f_i^{num} and f_i^{an} are the numerical and analytical solutions, respectively. The results in Fig.4 correspond to a shallower water case with kh=1.0, while Fig.5 is for deeper water with kh=6.283. For the FMM-BEM method, the errors on both the Dirichlet surface and Neumann surface are shown. The solution on the Neumann surface shows faster convergence than that on the Dirichlet surface in the shallower depth case (kh=1.0), while the opposite is seen with deeper water depth (kh=6.28). The errors of conventional constant BEM are not included in the comparison, since they are the same as that of FMM-BEM. The LPC and FVM methods show similar accuracy on the uniform rectangular meshes adopted in this study. However, separate numerical tests with FVM on distorted unstructured meshes showed unsatisfactory lower-order accuracy, which will not be shown here due to limited space. It is obvious from the comparison that the HPC method is the most accurate among the five methods in the comparisons.

The numerical details in each solvers used in the comparison, e.g. mesh arrangements, equation solvers and matrix preconditioners etc. may not be optimal. One can always be smarter to improve the numerical details to have a faster or more accurate solution, for instance, by using non-uniform/stretched elements on the vertical surface with smaller element size close to the horizontal surface y=0 and larger elements elsewhere. However, one will not be able to change the asymptotic behavior of the methods in terms of computational time.

In the next, we will show some time-domain results based on the LPC and HPC methods. In all the time-domain analysis presented in this paper, we have used a 4th order explicit Runge-Kutta scheme to integrate free-surface conditions in time. The method is first verified by studying a linear wave making problem. The normal velocity following the Airy's linear wave theory is prescribed at the position of the wave maker. Uniform grids in both horizontal and vertical directions are used in the analysis. Using only 15 unknowns per wave length ($\lambda = 15\Delta x = 15\Delta y$) gives very satisfactory results for both shallow and deep water depth cases compared with the analytical results. On the contrary, LPC method with the same mesh resolution does not seem to recover accurately the wave length. The numerical wave profile for a deep-water depth obtained by the LPC method with $\lambda = 20\Delta x = 20\Delta y$ is plotted in Fig.6 with gradual change of wave length away from the wave maker, indicating the wave dispersion errors [7]. We have also verified the HPC method for frequency-domain heave added mass and damping of a semi-submerged circular section.

The fully-nonlinear wave making problems are also studied. Because the free surface is a sharp interface within the context of potential flow theory, the surface tracking method is used to describe the free surface instead of the more time-demanding surface capturing techniques, such as the Volume of Fluid (VOF) method. The Lagrangian approach is applied to track the free-surface particle at the position of the wave maker, while a semi-Lagrangian approach is adopted elsewhere on the free surface. A body-fitted and free surface-fitted structured mesh, which is updated each time step, is used in all the analysis. Fig.7 shows the wave amplitudes of different harmonics along a wave tank. The piston wave maker is located at the left end of the tank while a numerical wave beach is applied on the other end. The stroke of the wave maker is 0.113m and the oscillation period of the wave maker is 3.5s. The water depth is 0.4m. According to linear wave maker theory, the generated wave amplitude and wave length away from the wave maker are A=0.042m and λ=6.78m, respectively. Therefore, we have the wave amplitude parameter $\alpha=A/h\approx0.105$, water depth parameter $\beta = h/\lambda \approx0.059$ and Ursell number $Ur=\alpha/\beta^2\approx30.2$. The numerical result shows good agreement with the experiments by Chapalain et al.[8]. For the same case, You & Faltinsen [9] have obtained equally good results by using a 3D fully-nonlinear BEM. Both the numerical results with and without a small Rayleigh damping are shown in the figure. It is also seen that, even though we used only 25% of the damping suggested by Chapalain et al.[8], we observed non-negligible damping effects on the higher-order harmonics. This indicates the necessity to find a more rational way of estimating the damping effect due to the boundary layers. For this non-breaking wave case, the turbulence at the free surface and the bulk viscosity of the water are not expected to be the dominant sources of damping. A linear boundary layer theory may be used to estimate the damping due to the boundary layers, as it is done in the sloshing tank [10].

The nonlinear monochromatic waves propagating over a submerged bar is also studied. The same problem was experimentally investigated by Luth et al [11]. We refer to Luth et al [11] for the details of the configuration of the tank and the submerged bar. Due to the limited pages, we only present the time history of the wave elevations at two points. One point is above the top surface of the bar and the other one is located near to the foot of the slope at the lee side. Fig.8 compares of the numerical wave elevation with the experiments. The wave period T=2.02s, wave amplitude A=0.01m and water depth h=0.4m were considered in the analysis.

As our future study, 2D floating bodies with vertical or non-vertical wall sides with nonlinear free-surface conditions will be studied by using the efficient HPC method. A Lagrangian approach should be used in satisfying the free-surface conditions near the body. To what extend we can model the overturning or nearly vertical free surface should be investigated. Since the 3D harmonic polynomials can easily be constructed, the HPC method will also be applied to 3D problems.

References:

[1]. Colicchio G, Greco M, Lugni C, Faltinsen, OM (2011) Towards a fully 3D domain-decomposition strategy for water-on-deck phenomena. Journal of Hydrodynamics. 22 (5), 462-467.

[2]. Kristiansen T, Faltinsen OM (2011) Gap resonances analyzed by a domain-decomposition method. In: Proceedings of 26th International Water Wave and Floating Bodies.

[3]. Wu GX, Eatock Taylor (1995) Time stepping solutions of the two-dimensional nonlinear wave radiation problem. *Ocean Engng.* 22(8), 785-798.

[4]. Liu YJ, Nishimura N. The fast multipole boundary element method for potential problems: a tutorial, *Engineering Analysis with Boundary Elements*, 30, No. 5, 371-381, 2006.

[5]. Theoretical Manual (2010). FINE™/Marine V2.2. NUMECA International.

[6]. Chung, TJ (2002). *Computational fluid dynamics*. Cambridge University Press.

[7]. Bingham HB, Zhang H. On the accuracy of finite difference solutions for nonlinear water waves. *J. Engineering Math.* 58, 211-228, 2007.

[8]. Chapalain G, Cointe R, Temperville (1992) Observed and modeled resonantly interacting progressive water-waves. *Costal Engineering*, 16, 267-300.

[9]. You J, Faltinsen OM (2012). A 3D fully nonlinear numerical wave tank for interaction between moored floating bodies and waves in shallow water. To appear in ISOPE 2012.

[10]. Faltinsen OM, Timokha AN (2009). Sloshing, Cambridge University Press.

[11]. Luth HR, Klopman G, Kitou N (1994). Kinematics of waves breaking partially on an offshore bar; LDV measurements of waves with and without a net onshore current. Report H-1573, Delft Hydraulics.

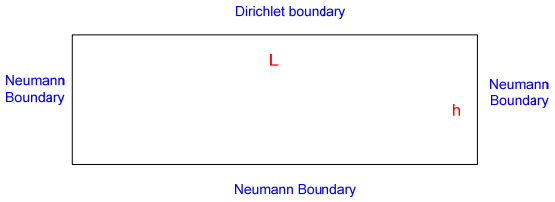

Fig.1.Definition of the 2D rectangular box.

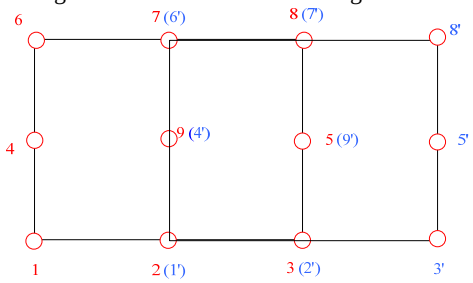

Fig.2. Sketch of 2 neighbor cells used in LPC and HPC methods.

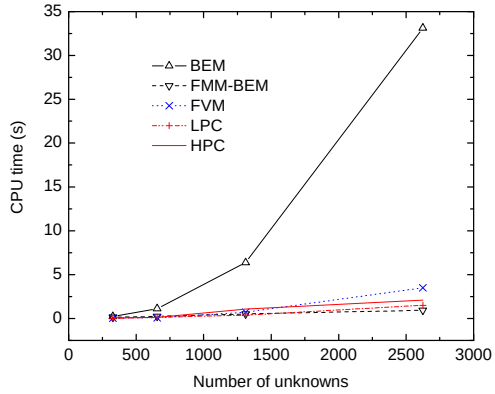

Fig.3. Comparison of CPU time.

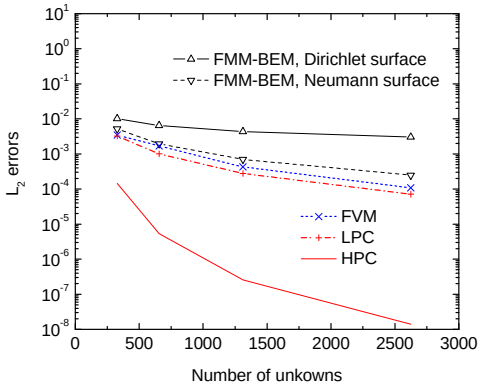

Fig.4. Comparison of L_2 errors. kh=1.0.

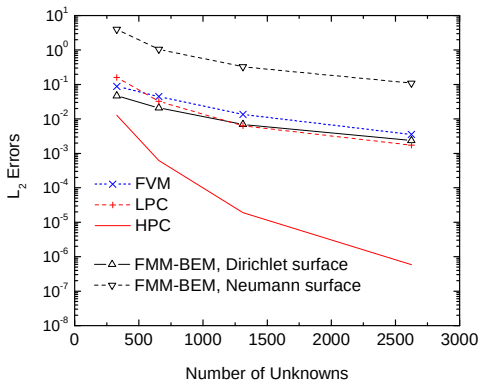

Fig.5. Comparison of L_2 errors. kh=6.28.

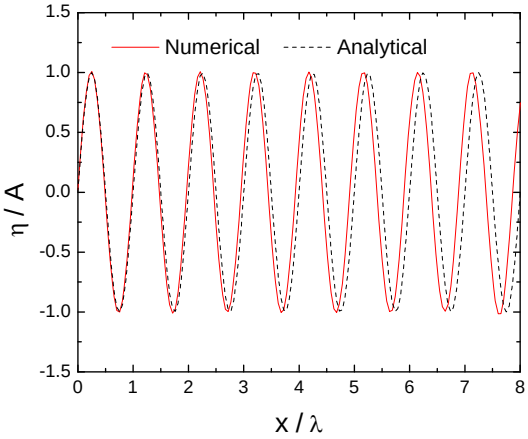

Fig.6 Wave profile by LPC method. λ=20Δx=20Δy.

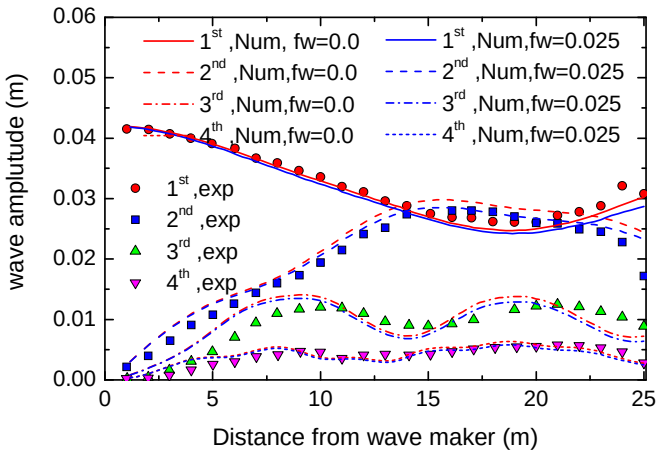

Fig.7. The wave amplitude for different harmonics along the tank.

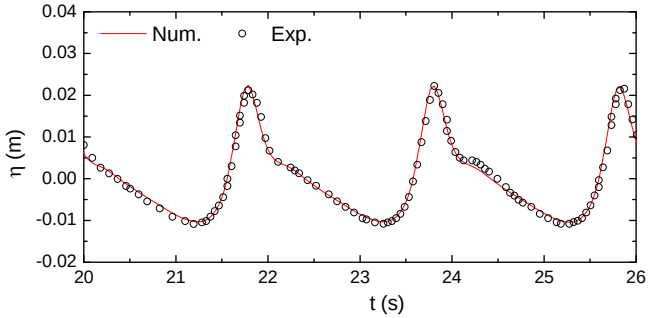

Fig.8a. Wave elevation at x=12.5m

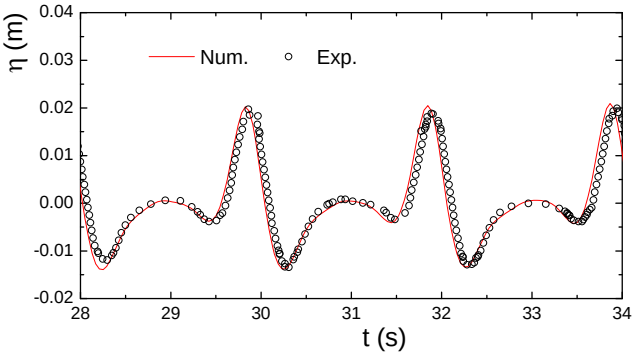

Fig.8b. Wave elevation at x=17.3m.